Available online at www.sciencedirect.com
SCIENCE DIRECT®
Journal of Power Sources 137 (2004) 43–52
JOURNAL OF POWER SOURCES
www.elsevier.com/locate/jpowsour

The effect of reservoirs and fuel dilution on the dynamic behavior of a PEMFC

Sunhoe Kim, S. Shimpalee, J.W. Van Zee*

Department of Chemical Engineering, University of South Carolina, Columbia, SC 29208, USA

Received 23 April 2004; accepted 15 May 2004
Available online 10 August 2004

Abstract

Data are presented to characterize the effects of reservoir size and hydrogen dilution on the dynamic behavior of a proton exchange membrane fuel cell (PEMFC) subjected to rapid changes in the voltage when the flowrates are constant. The data consist of the responses of the current density during low fuel stoichiometries in an effort to expand an understanding of the previously observed overshoot/undershoot behavior. That is, recent studies of the dynamic behavior of a PEMFC have shown pseudo-second-order dynamics of the current response to a change in voltage [J. Power Sources (2004); J. Electrochem. Soc. (2004)]. The data reported here lend further evidence that under fuel starved conditions, rapid changes in the cell voltage between 0.7 and 0.5 V yield pressure differences sufficient to create a "vacuum" effect. This vacuum effect may cause fuel to be drawn from the manifold in a stack or cause ambient air to enter a laboratory scale cell. The vacuum effect explained in our previous work [J. Power Sources (2004)] is shown here to depend on diameter and volume of fuel reservoirs and on the concentration of hydrogen in the fuel.

Keywords: PEM fuel cells; Electric vehicle; Transient behavior; Dynamic behavior; Reservoir effect; Dilution effect

1. Introduction

As discussed previously [1,2], transient operation of PEMFCs during stationary and automotive applications may be a result of a sudden demand as an appliance starts or as a vehicle is accelerated or decelerated. Further these transients may be of sufficient magnitude and speed that gas flowrates cannot be adjusted by feedback control or that the capacitors in the system cannot accommodate the demand. We recently showed that these transients result in pseudo-second-order dynamics in the current response when the voltage was changed during operation with low fuel stoichiometry in a 25 cm^2 laboratory cell. We believe these transients expose the MEA to various degrees of stoichiometry and distributions of the current density, temperature, and water as predicted recently, by three-dimensional simulations presented by Shimpalee et al. [3,4]. Here we present experimental data for this second-order response of the current that shows both the effects of a fuel reservoir and the effects of diluting the hydrogen fuel with nitrogen.

The objective of this paper is to test two hypotheses by presenting an experimental study of the second-order dynamic behavior observed during changes in the voltage. The terms and definitions used for this study are shown in Fig. 1a and b for an idealized forcing function and response. During an increase in the load at a fixed set of anode and cathode flowrates, the voltage is changed from a high value to a low value (e.g., 0.7–0.5 V in Fig. 1a). This change results in an increase in the measured current and if we use the geometric area we can obtain a response such as that shown for the current density. This response may overshoot the final value of the current density value due to residual hydrogen in the cell and the degree of overshoot can be labeled "*O*" in Fig. 1a. Then we typically observe a period of time before the current starts to decrease and we label this time as the "Peak Length." The overshoot "*O*" may then be followed by an undershoot "U_o" [1,2]. On the other hand, as shown in Fig. 1b, we observed an undershoot "U_u" without an overshoot when we change the cell voltage from 0.5 to 0.7 V for a starved condition. Fig. 1a and b also shows gains, K_1 and K_2, used in the mathematical analysis as discussed below.

One of the hypotheses to be tested here is a result of observations in references [1,2]. There we suggested that the "U_o" was due to a "vacuum" effect dependent on the velocity

* Corresponding author. Tel.: +1 803 777 2285; fax: +1 803 777 8142.
E-mail address: vanzee@engr.sc.edu (J.W. Van Zee).

0378-7753/$ – see front matter © 2004 Elsevier B.V. All rights reserved.
doi:10.1016/j.jpowsour.2004.05.035

Nomenclature

i	current density (A/cm^2)
K	steady state gain (A/cm^2 V)
t	time (s)
V	cell voltage (V)
ΔV	cell voltage difference (V)

Greek letters

β	lead time constant (s)
δ	time constant for cell voltage (s)
ξ	damping coefficient
ρ	lead-to-lag ratio ($\rho = \beta/\tau$)
τ	time constant (s)

of the fuel in the flow channels. That is, undershoot behavior is not observed when a single path flow channel is used because the faster exit velocity of hydrogen decreases the amount of air that penetrates the cell. On the other hand, "U_o" was observed when a triple path flow field is used because the velocity in each channel is less thereby allowing more ambient air to enter the cell [2]. Also a larger fraction of the MEA is exposed to air when a triple path flow field is used because the air can enter three channels. It is important to note also that the undershoot discussed here follows an overshoot and that it is therefore fundamentally different than the undershoot observed when the cell voltage is increased. That undershoot appears to be a result of the current distribution becoming more uniform as the load is decreased and as the apparent stoichiometry is increased [3,4]. Thus, to test this first hypothesis, we used diluted fuel to change the velocity in a triple path flow field cell so that comparisons could be made at the same stoichiometry.

The second hypothesis to be tested here also involves the "vacuum" effect but it relates to the peak length in Fig. 1a. We hypothesize that the peak length can be increased or decreased depending on the volume and diameter of a hydrogen reservoir at the exit of the cell. This reservoir may be a model for part of the manifold in a stack of cells and our

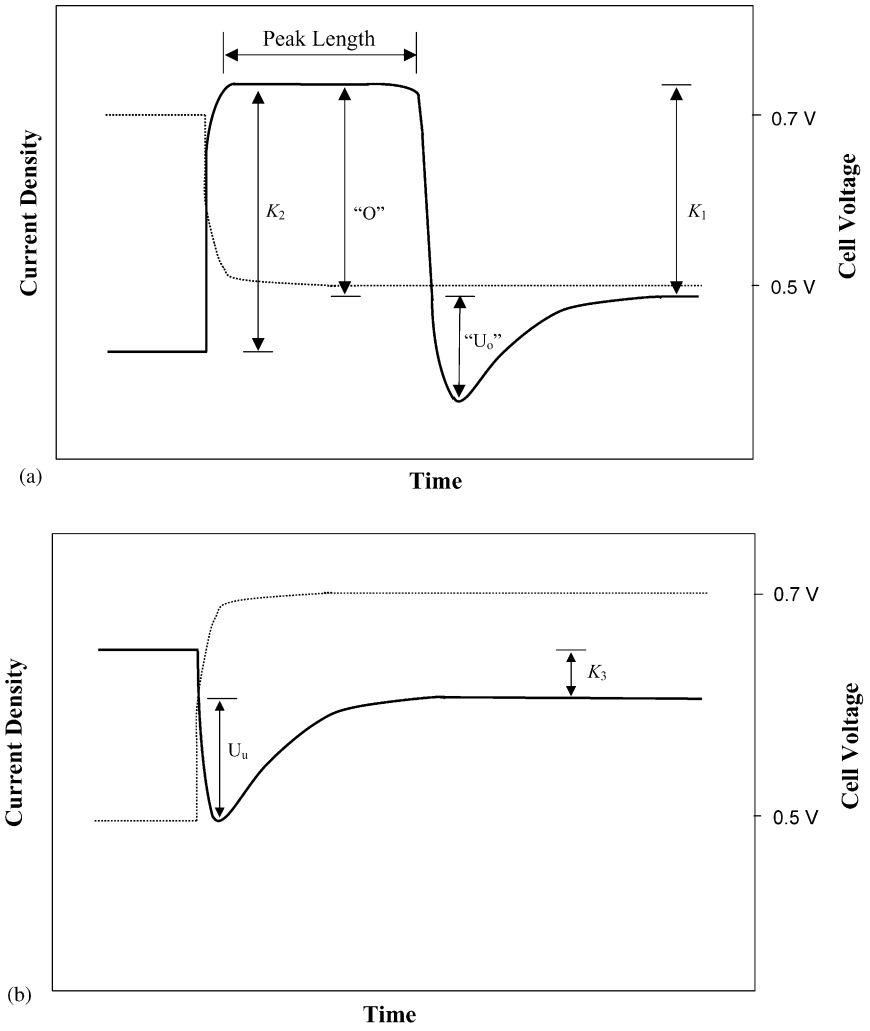

Fig. 1. (a) Schematic of overshoot-"undershoot" behavior during a voltage change from 0.7 to 0.5 V at fixed flow rates: (---) cell voltage and (—) current density. (b) Schematic of undershoot behavior during a voltage change from 0.5 to 0.7 V at fixed flow rates: (---) cell voltage and (—) current density.

focus here is to study the interaction of this "vacuum" effect and the manifold size by isolating a single cell. The hypothesis includes the diameter of the reservoir because, again, we want to test the concept that velocity at the exit is a major effect for the overshoot/undershoot behavior. Thus a manifold with more hydrogen should have a longer peak length and the depth of the resulting undershoot should be a function of reservoir diameter since the "vacuum" effect is influenced by the velocity of the fuel flowing into the channel.

Our reviews of the literature [1,2] indicate that experimental analysis of the behavior in Fig. 1a and b are new for PEMFCs. On the other hand, there have been studies on system performance of PEMFC stacks [5] and battery–PEMFC hybrid systems [6–8]. In Reference [1] we considered the effect of stoichiometry on the dynamics behavior and we showed that for fixed flowrates, voltage changes yielded current densities that could be described by a simple first-order decay or increase:

$$i(t) = i(t=0) + K\,\Delta V(1 - \mathrm{e}^{-t/\tau}) \tag{1}$$

when those changes resulted in stoichiometries that changed from excess conditions to a 1.2/2.0 condition for hydrogen and air, respectively. On the other hand, the overshoot and "undershoot" behavior, illustrated in Fig. 1a, occurs when the voltage change results in a stoichiometry change from 1.2/2.0 to a 'starved' condition. This behavior was classified as a second-order lead/lag (SO L/L) response system and described by Eqs. (2a)–(2c) below [1]:

$$\tau^2 \frac{\mathrm{d}^2 i_1}{\mathrm{d}t^2} + 2\xi\tau \frac{\mathrm{d}i_1}{\mathrm{d}t} + i_1 = K_1[V(t) - V(t=0)] \tag{2a}$$

$$i_2 = K_2\,[V(t) - V(t=0)] \tag{2b}$$

$$i(t) = i_1(t) + i_2(t) \tag{2c}$$

Thus transient behavior after the peak was described by the second-order differential equation for i_1 and the initial peak in the current density, i_2, was described by the product of a constant gain, K_2, and the voltage difference. In Reference [1] the peak length was ignored and this resulted in some lack of fit. Here we include the peak length, as discussed below, and the fit is improved. The undershoot behavior shown when the stoichiometry changes from a 'starved' to a normal condition, illustrated in Fig. 1b, can be classified as a first-order lead/lag (FO L/L) system [1,9]:

$$i(t) = i(t=0) + K_3[1 - (1-\rho)\mathrm{e}^{-t/\tau}][V(t=0) - V(t)] \tag{3}$$

2. Experimental

The same single cell PEMFC and MEA from our other work [1,2] was used for these experiments. The MEAs were PRIMEA® Series 5510 MEA (0.4 mg/cm^2 Pt loading, 25 μm nominal membrane thickness, W.L. Gore & Associates Inc. Elkton, Maryland, USA). The original active electrode area was 25 cm^2. The active reaction area of the MEA is reduced from 25 to 20 cm^2 by sub-gaskets for both anode and cathode sides. The gas diffusion layers (GDLs) used in this work were CARBEL™ CL (16 miles = 0.41 × 10^{-3} m of nominal thickness produced by W.L. Gore & Associates Inc. Elkton, Maryland, USA). The cell was tightened with eight volts with equivalent torques of 50 lb$_f$ in./bolt. This was determined previously to give the optimal degree of internal compression according to the experiments of Lee et al. [10].

A triple serpentine flow field (SFF) was used in this experimental paper to investigate the length of peak and the "undershoot" after overshoot. The electrical load to control the cell voltage was a Model 6060B (Agilent Technologies) that had a capability of 60 A and 300 W. The fuel cell test station used to control the electrical load, inlet fuel flowrates, and cell and humidity bottle temperature was a product of Fuel Cell Technology (Los Alamos, NM). The digital mass flow controllers (MKS), which were calibrated by bubble flow meters as discussed in reference [11], were used to control the fuel and air flowrates. The inlet hydrogen and air pass through the humidity bottles to be heated and humidified. The humidity of the inlet flows is determined by using previously obtained calibration curves at fixed temperatures of the humidity bottles. In the data reported here we estimate the dew point temperatures of anode and cathode to be 80 and 70 °C, respectively. The hydrogen and air enter into the cell in co-current flow and diffuse through the GDLs to reach the electrode where electrochemical reaction takes place. Usually the non-reacted gas and air exit the cell, pass through the backpressure regulators and then through lengths of tubing that can be considered reservoirs before they are vented. Note that these regulators are not check values and the outlets of hydrogen and air are open to the atmosphere in this work because the backpressures of both the anode and cathode sides were set to atmospheric pressure, 101 kPa. The gases in this experimental work were high purity hydrogen (99.997%) and industrial grade compressed air.

Prior to performing the transient experiments the steady state performance was measured to establish a well humidified MEA baseline with different concentrations of hydrogen (i.e., 100, 80, and 40%) diluted with nitrogen while keeping a stoichiometry of 1.2 and 2.0 for the anode and cathode, respectively. The stoichiometry 1.2/2.0 corresponds to flowrates that were 1.2 times greater than required (by the measured current) for hydrogen and 2.0 greater than that required on the cathode for air. The polarization curves were obtained at the cell voltage from 0.45 V to open circuit voltage (OCV) in 0.05 V randomized steps to insure that no hysteresis is included with the reported polarization curves. The constant stoichiometry requires different flowrates, according to current, for each cell voltage and these flowrates were adjusted manually in an iterative manner according to measured current to maintain the fixed stoichiometry. Note that, for example, if the hydrogen requirement is 80 cm^3/min, for 80% hydrogen in mixture gas, the total flowrates of the mixture gas is 100 cm^3/min.

Table 1
Overshoot and undershoot comparison for dilution effect when $\Delta V = 0.2$ V at $V(t = 0) = 0.7$ or 0.5 V

	Voltage change (V)	Stoichiometry		Current density at $t = 0$ (A/cm^2)	Peak or minimum current density (A/cm^2)	Change in current density (A/cm^2)	Current density at $t = \infty$ (A/cm^2)	Recovery time from undershoot (s)	Flow rates, A/C (cm^3/min)
		$t = 0$	$t = \infty$						
Neat H_2	0.7–0.5	1.2/2.0	1.0/1.7	0.49	0.79	$O = 0.28$	0.51	N/A	86/357
	0.5–0.7	1.0/1.7	1.2/2.0	0.51	0.32	$U_u = 0.17$	0.49	5.8	86/357
80% H_2	0.7–0.5	1.2/2.0	1.0/1.7	0.40	0.69	$O = 0.27$	0.42	N/A	89/295
	0.5–0.7	1.0/1.7	1.2/2.0	0.42	0.30	$U_u = 0.10$	0.40	2.2	89/295
40% H_2	0.7–0.5	1.2/2.0	1.0/1.7	0.35	0.62	$O = 0.20$	0.40	N/A	155/258
	0.5–0.7	1.0/1.7	1.2/2.0	0.40	0.28	$U_u = 0.07$	0.35	1.0	155/258

Linear approximated voltage changes are 0.22 V/s for all cases.

A two channel digital oscilloscope (TDS 210, Tektronix Inc.) was used to record simultaneously both the current response and the voltage forcing function as illustrated in our previous work [1]. The current was recorded in a form of a voltage signal, via a "hall effect" current sensor at the first channel of the oscilloscope. The cell voltage was measured directly at the cell's current collector plates and then recorded in second channel of the oscilloscope. For the cell voltage changes from 0.7 to 0.5 V in this work, the test station, computer interface, and electronic load bank limited the rate of voltage change to be about 0.2 ± 0.05 V/s. This approximate rate can be calculated as a linear change from 0 to t (s) corresponding to the time, t, when the voltage crosses 0.5 V. In actuality, the cell voltage change rate was non-linear and it can be characterized best with a first-order exponential response [1,2]:

$$V(t) = V(t = 0) + \Delta V(1 - e^{-t/\delta}) \quad (4)$$

where ΔV is cell voltage difference (-0.2 V for the voltage change from 0.7 to 0.5 and 0.2 V for from 0.5 to 0.7 V), and the time constant, δ, is equal to 0.4 s for the data shown in this paper.

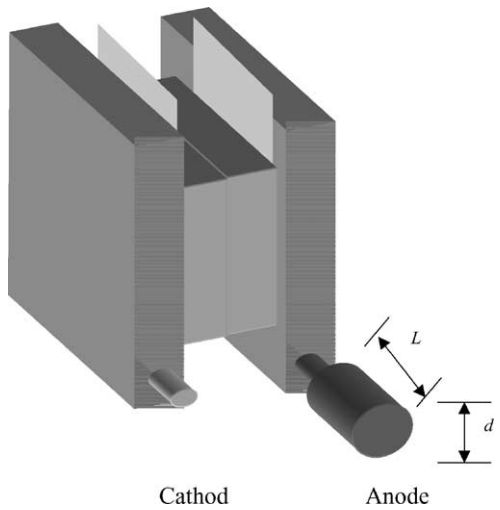

Fig. 2. Schematic diagram of experimental setup for reservoir effect experiment. There are three different volumes of reservoirs and six different lengths corresponding to the three reservoir volumes of Table 2 (i.e., 5, 10, 15 cm^3).

The dilution effect was measured with three different hydrogen/nitrogen mixture concentrations (100, 80, and 40% hydrogen) at a stoichiometry of 1.2 and 2.0, for the anode and cathode, respectively. There are two cases for the dilution effect experiments, corresponding to $\Delta V = -0.2$ V and $\Delta V = 0.2$ V yielding overshoot and undershoot behaviors, respectively. Note that the stoichiometry changed from a normal to a 'starved' conditions and from a 'starved' to a normal conditions depending on ΔV and $V(t = 0)$ for the constant inlet flowrates shown in Table 1.

The "reservoir" was constructed at the exit with tubes of different sizes to study the overshoot peak length. Three volumes of tube (5, 10, and 15 cm^3) were used in this work. Also, there were two different diameters of the tubes and the volumes were adjusted by cutting the length of the tube. The outer diameters of the tubes were nominally 0.64 and 1.27 cm and the inner diameters were 0.46 and 0.95 cm, respectively. Fig. 2 illustrates the schematic diagram of the experiment setup for the reservoir effect. The details of the sizes and diameters are discussed with the results below. In addition to these reservoir sizes, the volume of the cell may be of interest and it is calculated based on the channel volume, GDL's thickness and porosity, and the actual 25 cm^2 of the cell. The channel volume is the multiplication of depth of 0.07 cm, width of 0.1 cm, and length of 66 cm and there are three channels in the triple path serpentine flow field. This yields a channel volume of 1.39 cm^3. Also, the GDL volume was 1.02 cm^3 based on the 25 cm^2 area, the 16 mils thickness (i.e., 0.0406 cm), and the porosity of 0.7. Thus the total volume inside of the cell is 2.4 cm^3.

3. Results and discussion

We conducted the experiments for quantifying the overshoot behavior of PEMFC. These data are best described after a typical overshoot/undershoot response is analyzed (Fig. 1a) and after a typical undershoot response is analyzed (Fig. 1b). It is important to note that as discussed in previous papers [1,2] the overshoot/undershoot behavior and the undershoot behavior occur only for starved conditions. Fig. 3 was shown as a guide to the normal steady state voltage/current behavior for fixed flowrates corresponding to a

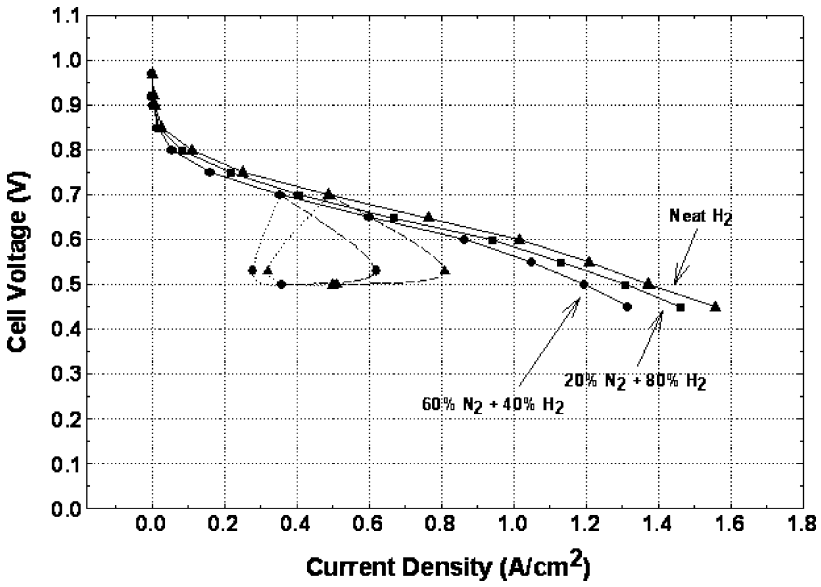

Fig. 3. Polarization behaviors of a PEMFC for various concentrations of hydrogen. The cell temperature of 70 °C. The dew point temperatures of anode and cathode are 80 and 70 °C. The dashed lines (---) indicate that the approximate path of the current during the overshoot behavior as the cell voltage is changed from 0.7 to 0.5 V. The dotted line (· · ·) indicates that the approximate path of the current during the undershoot behavior as the cell voltage is changed from 0.5 to 0.7 V.

1.2/2.0 stoichiometry. The dashed lines indicate that the approximate path of the current during the overshoot behavior as the cell voltage is changed from 0.7 to 0.5 V. The dotted line indicates that the approximate path of the current during the undershoot behavior as the cell voltage is changed from 0.5 to 0.7 V. When, as a result of the voltage decrease (the independent variable), the current (a dependent variable) increases to its limit at a fixed flowrate, the stoichiometry (a dependent variable for fixed flowrates) changes from the normal to the 'starved' condition, and an overshoot behavior was observed. The normal condition defined in this experimental work is 1.2 and 2.0, anode and cathode, respectively. Note that because we are controlling the voltage, the stoichiometry can never be truly 'starved' since the current will respond to the applied voltage and the availability of reactant. However, we use the term 'starved' to indicate the condition when the current corresponds to a stoichiometry close to 1.0.

Fig. 4a and b shows the dimensional and dimensionless comparison of overshoot behavior with different concentrations of hydrogen for the case when there is no reservoir. The dimensionless comparison is useful because these dilution effect experiments have different initial current densities and thus it is difficult to compare changes in the current densities directly. Thus, we introduce the dimensionless current density which is obtained by dividing the transient current density by the respective steady state value $t = \infty$. These current densities at $t = 0$ and $t = \infty$ are listed in Table 1. In Fig. 4a, the overshoot peaks for neat hydrogen, 80, and 40% of hydrogen are about 0.79, 0.69, and 0.62 A/cm^2, respectively. As shown in Fig. 4b, the dimensionless magnitude of the overshoot is independent of hydrogen concentration. For the neat hydrogen case the overshoot peak length is approximately 2.0 s, while for the diluted hydrogen the peak length was zero. The current density with 40% hydrogen decreased the fastest and this is consistent with less hydrogen in the flow channel and GDL. Also, the dimensionless value of U_o is largest for neat hydrogen and we argue that the apparent undershoot for the diluted gases is really a function of the inability of the load to precisely control the cell voltage during the first 2.5 s. As discussed in our previous work [1], the "undershoot" after overshoot peak is a result of air flowing back into the cell at the end of the anode. To check this hypothesis, we attached a u-shaped site tube filled with a soap-bubble solution at the anode exit and we observed bubbles flowing away from the cell during operation with diluted fuel. We observed the bubbles moving towards the cell during operation with neat hydrogen. The dimensional current density, values of overshoot peak, and stoichiometries are listed in Table 1.

Fig. 5a shows the comparison of undershoot behavior for the different concentration of hydrogen fuel. The undershoot behavior in this figure corresponds to U_u from Fig. 1b and it occurs when the fuel supply condition is changed from a starved to a normal condition. The minimum current density at the undershoot depths for neat, 80, and 40% hydrogen concentrations are 0.32, 0.30, and 0.28 A/cm^2. The dimensionless values of undershoot are different for each case (i.e., Fig. 5b). However, the current density recovery times are different. The recovery times for 100, 80, and 40% hydrogen are approximately 5.8, 2.2, and 1.0 s, respectively. The more dilute the hydrogen, the faster the current density recovers. This can be explained if there is a non-uniform distribution

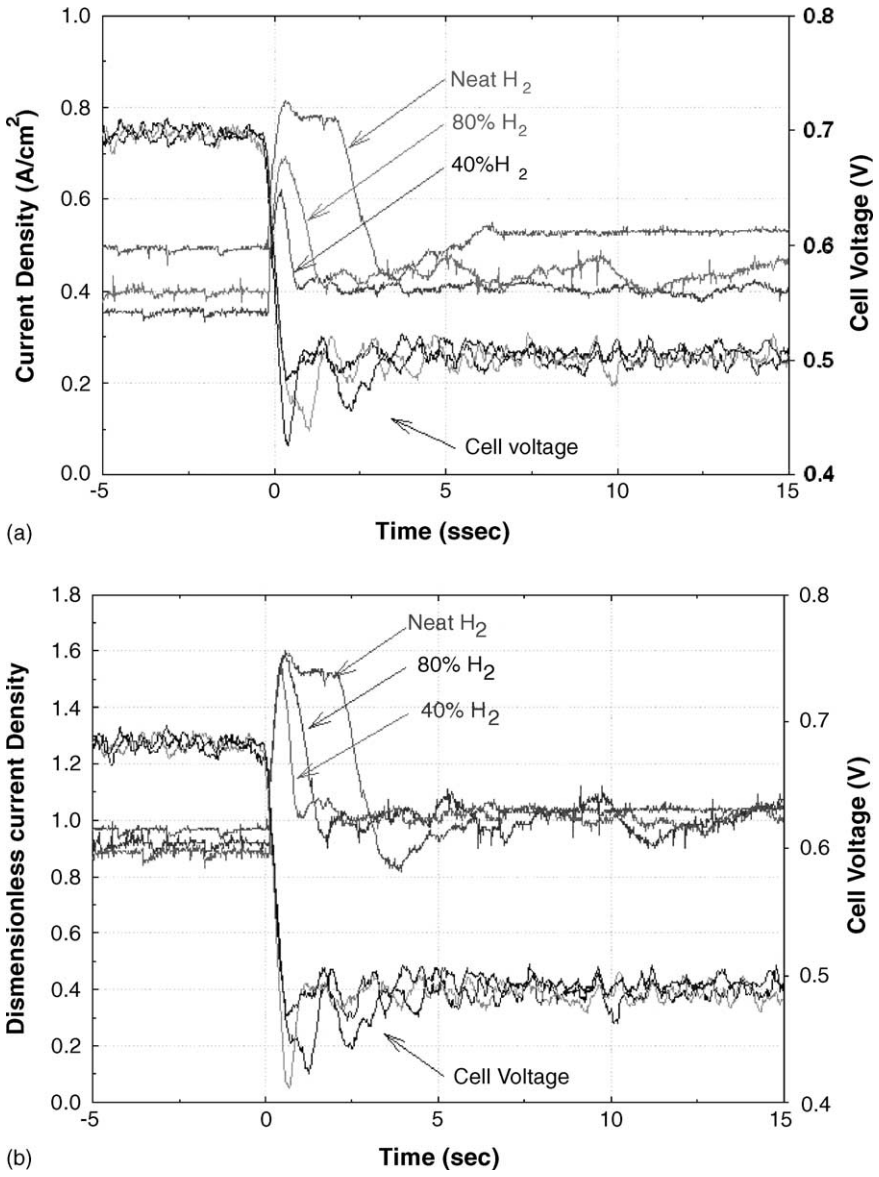

Fig. 4. (a) Comparison of dilution effects on overshoot behavior for different concentrations of hydrogen, neat, 40, and 80% diluted with nitrogen. Here, the resulting fuel stoichiometry condition changes from a normal condition to a starved. (b) Dimensionless comparison of dilution effects on overshoot behavior for different concentrations of hydrogen, neat, 40, and 80% diluted with nitrogen. Cell Voltage changes from 0.7 to 0.5 V.

of current density at the beginning of the cell so that the higher velocities due to the dilution of the fuel lead to faster replenishment of hydrogen throughout the cell, which yields faster recovery. The values of the undershoot recovery time and the minimum currents are listed in Table 1.

The parameters in Eqs. (2a)–(2b) that yield a good fit for the SO L/L model system are listed in Table 2. Note that for the neat hydrogen the R^2 is lower because we applied Eq. (2a) from the time the peak current was obtained and thus we neglect a parameter for the peak length in a manner consistent with reference [1]. Note that the parameters in the table are based on dimensionless current density. The gain K_2, represents the overshoot peak current density relative to the current density at $t = 0$ as shown in Fig. 1a. The other gain, K_1, corresponds to the current density decay from the peak to final current density values. The undershoot following the overshoot peak that were observed in the neat hydrogen case were affected by damping coefficients, ξ, as

Table 2
Parameters for the dimensionless overshoot SO L/L system for dilution effect experiment

	Gains (V^{-1})		Time constant, τ (s)	Damping coefficient, ξ	R^2
	K_1	K_2			
Neat H_2	3.1	−3.1	1.0	0.6	0.915
80% H_2	2.8	−3.2	0.6	0.8	0.947
40% H_2	2.4	−2.9	0.4	0.8	0.950

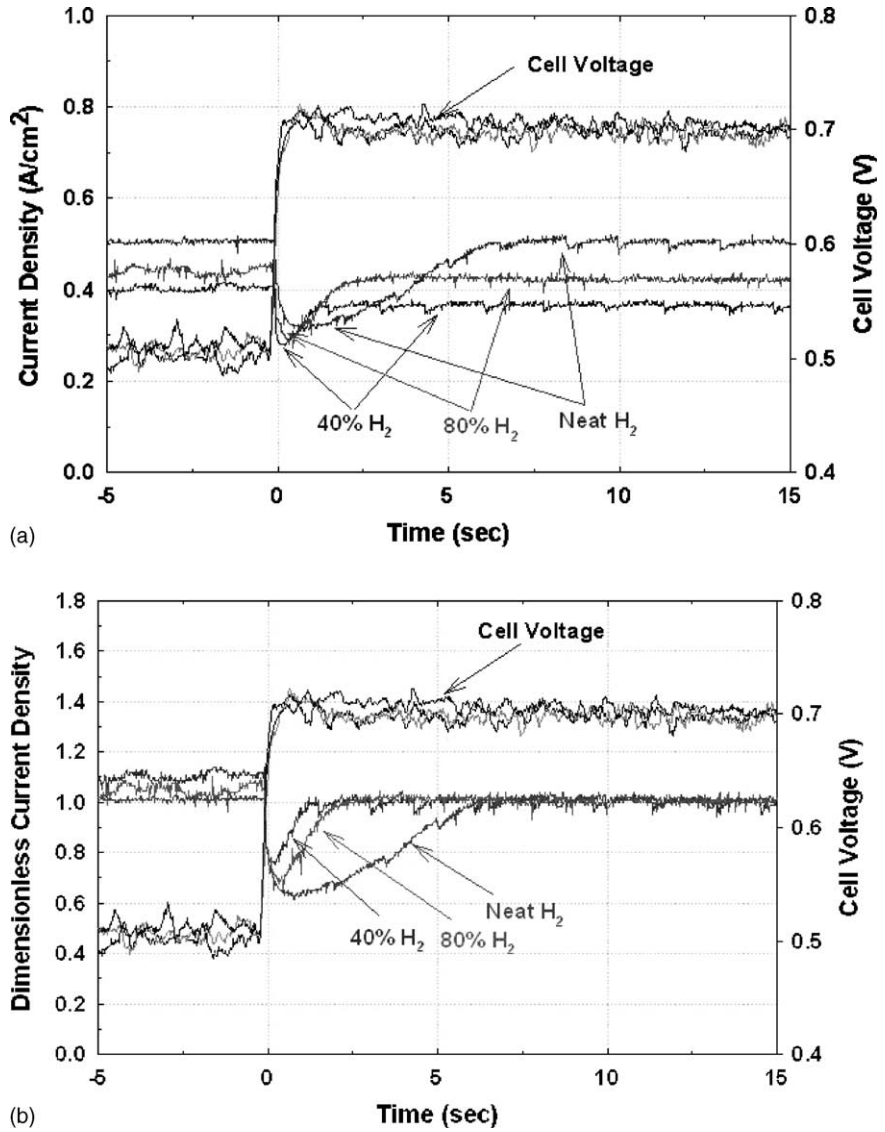

Fig. 5. (a) Comparison of dilution effects on undershoot behavior for different concentrations of hydrogen, neat, 40, and 80% diluted with nitrogen. Here, the resulting fuel stoichiometry condition changes from a starved to a normal condition. (b) Dimensionless comparison of dilution effects on undershoot behavior for different concentrations of hydrogen, neat, 40, and 80% diluted with nitrogen. Cell Voltage changes from 0.5 to 0.7 V.

explained in reference [1]. Also, the time constants, τ, for each case affect the current decay after the overshoot peak. The time constants were obtained from experimental data in the same manner discussed in our previous work [1]. The corresponding parameters for Eq. (3), a FO L/L system, are listed in Table 3. The gain, K_3, and lead to lag ratio, ρ, determine the instantaneous undershoot peak and the time constant, τ, determines the rate of recovery to the final steady state value. These values were obtained using MATLAB Simulink® from experimental data as explained in our previous work [1]. The gain K_3 is illustrated in Fig. 1b. Again, these parameters were calculated based on dimensionless current density data.

Table 3
Parameters for the dimensionless undershoot behaviors FO L/L system for dilution effect

	Gain, K_3 (V^{-1})	Lead time constant, τ (s)	Lag time constant, β (s)	R^2
Neat H_2	−0.2	3.0	38	0.959
80% H_2	−0.3	1.2	11	0.980
40% H_2	−0.5	0.8	3	0.973

Fig. 6 shows the effect of a reservoir connected at the end of the anode as illustrated in Fig. 2. Neat hydrogen was used in this experiment. Note that the cell voltages shown in the figure indicate that the cell voltage change rates were the same for all cases. Data for four experiments are shown in this figure corresponding to four volumes: Vol. = 0 cm^3 (i.e., without reservoir tube) and Vol. = 5, 10, and 15 cm^3. The overshoot peak is approximately 0.79 A/cm^2 for all cases when the cell voltage is 0.5 V. This value of the current

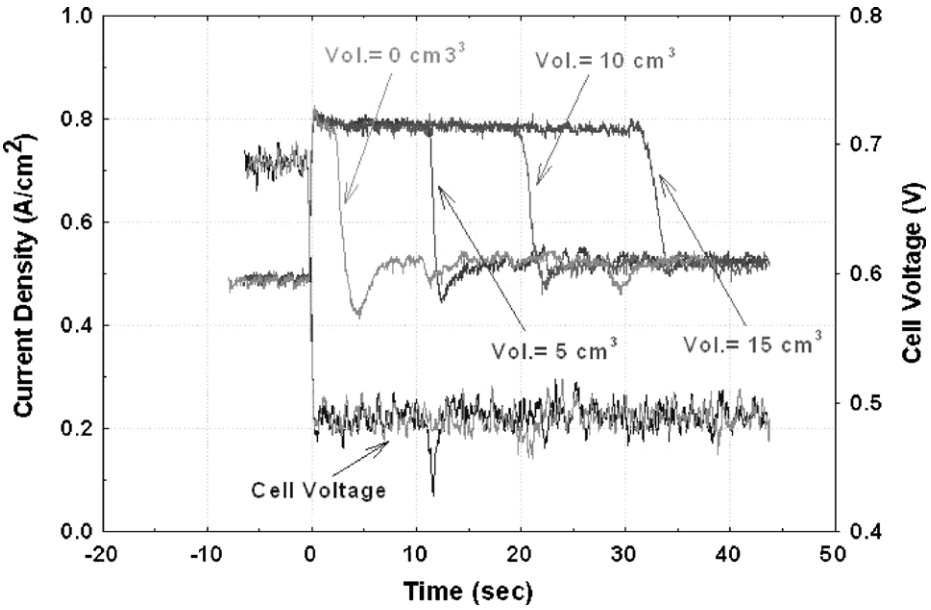

Fig. 6. Comparison of overshoot peak length and "undershoot" with three different volumes of 5, 10, and 15 cm^3, of reservoir tubes with quarter inches of outer diameter (inside diameter of 0.46 cm).

density in the overshoot peak is lower than what would be expected for a stoichiometry of 1.2/2.0 shown in the polarization curve because the cathode stoichiometry is actually 1.7 at this flowrate [1]. The lowest "undershoot" current density is about 0.42 A/cm^2, after this "undershoot" the current density increases, and reaches a steady state value for the case without reservoir. The "undershoot" current density peak for the reservoir sizes of 5, 10, and 15 cm^3 are 0.43, 0.45, and 0.48 A/cm^2, respectively. The values of "U_o" corresponding to Fig. 1a are 0.10, 0.09, 0.07 and 0.04 A/cm^2 for the 0, 5, 10 and 15 cm^3 volumes of the reservoir tube, respectively. The flowrates in these experiments are 86 and 357 cm^3/min for the anode and cathode, respectively. Note that the flow condition at 0.7 V corresponds to stoichiometries of 1.2/2.0 and that at 0.5 V these conditions correspond to stoichiometries of 1.0/1.7. The current density at 0.5 V with these flowrates corresponds to a starved condition, and thus there are some small oscillations as discussed in our previous work [1]. For Fig. 6, the volume of the reservoir is determined with the tube length and one can observe that the bigger reservoir volume yields a longer overshoot peak as expected. Also, the "undershoot" after overshoot behavior is less with longer reservoir tubes as is consistent with the hypothesis that the "undershoot" is caused by ambient air entering the cell. The peak length and reservoir sizes are listed in the Table 4 and one will note that the theoretical peak length is longer than that of actual experimental result. This theoretical peak length is calculated assuming plug flow conditions with the volume of flow channel, GDL, and reservoir sizes and one explanation for the difference is that the reservoir does not

Table 4
Peak length and "undershoot" comparison in the cell voltage changes from 0.7 to 0.5 V with flow rates of 86/357 cm^3/min, neat hydrogen and parameters for the SOPDT for reservoir effect

Tube volume (cm^3)	Tube diameter	Tube length (cm)	Stoichiometry		Peak length (s)	"Undershoot" depth (A/cm^2)	Velocity in reservoir (cm/s)	Damping coefficient, ξ	Time delay, α (s)	R^2
			$t = 0$	$t = \infty$						
0		0.00	1.2/2.0	1.0/1.7	2.0	0.42	–	0.6	0	0.913
5	1/2 in. o.d.	7.02	1.2/2.0	1.0/1.7	6.1	0.44	0.34	0.6	6	0.995
	1/4 in. o.d.	30.45	1.2/2.0	1.0/1.7	11.1	0.43	1.48	0.6	10	0.988
10	1/2 in. o.d.	14.03	1.2/2.0	1.0/1.7	9.1	0.48	0.34	0.6	11	0.998
	1/2 in. o.d.	60.90	1.2/2.0	1.0/1.7	19.4	0.45	1.48	0.6	19	0.992
15	1/2 in. o.d.	21.04	1.2/2.0	1.0/1.7	13.3	N/A	0.34	0.6	15	0.995
	1/4 in. o.d.	91.35	1.2/2.0	1.0/1.7	31.4	0.48	1.48	0.6	32	0.996

Calculated peak lengths for tube volume of 0, 5, 10, 15 cm^3 are 2.90, 15.1, 27.3 and 39.5 s, respectively; overshoot peak is 0.79 A/cm^2. Initial and final current density is 0.49 and 0.51 A/cm^2, respectively. Gains for all cases are 1.6 and −1.6 (A/cm^2 V) for K_1 and K_2, respectively. Time constant, τ, for all cases is 1.0 s.

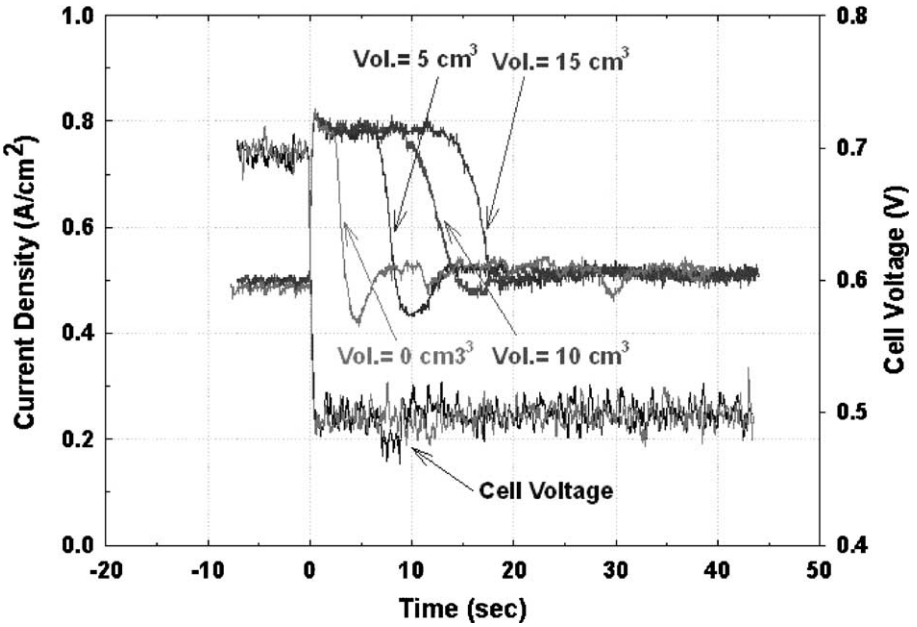

Fig. 7. Comparison of overshoot peak length and "undershoot" with three different volumes of 5, 10, and 15 cm^3, of reservoir tubes with half inch outer diameter (inside diameter of 0.95 cm).

empty into the cell as plug flow but rather some ambient air also enters the cell because the boundary between hydrogen and ambient air is not clear at the end of the reservoir tube.

Fig. 7 shows the response for reservoirs with a bigger diameter tube (i.e., the inner diameter is 0.95 cm for the 1/2" o.d. tube) for the same three volumes as in Fig. 6. As mentioned in the previous figure, the theoretical peak lengths shown in Table 4 are longer than those of actual experiment but this difference is more significant with the bigger diameter tubes. Again, this may be a result of deviations from plug flow and this deviation also explains the more pronounced "undershoot" with the larger diameter tubes. The peak is the same as that in Fig. 6, about 0.79 A/cm^2. The value of the "undershoot" for the 5 cm^3 of reservoir tube is 0.44 A/cm^2, for the 10 cm^3 of reservoir tube is 0.48 A/cm^2, and for the 15 cm^3 the "undershoot" is barely observable in the figure. The values of "U_o" corresponding to Fig. 1a are 0.09, 0.03, and 0 A/cm^2 for the 5, 10 and 15 cm^3 volumes. The current density values of $t = \infty$ approaches the same value,

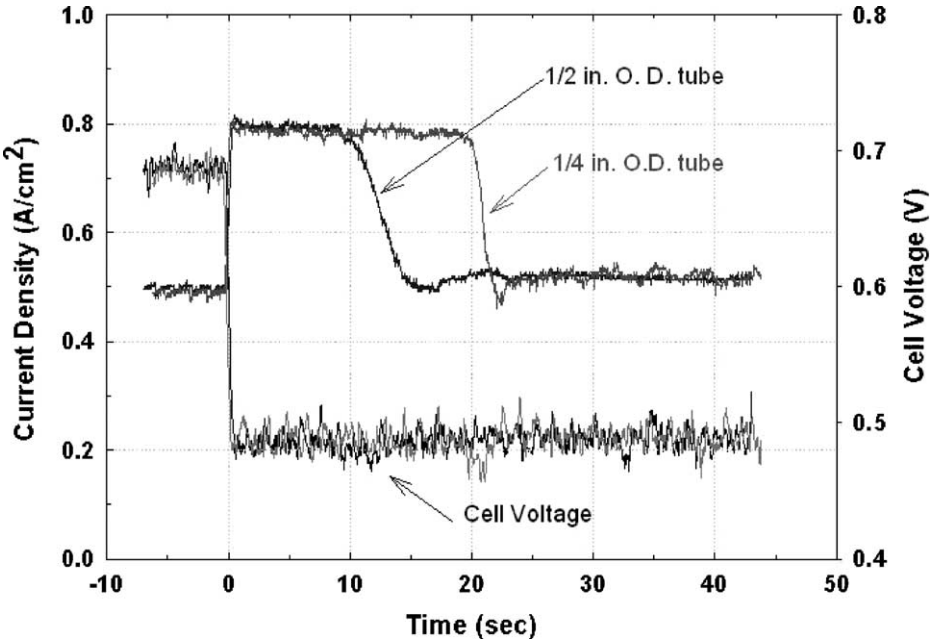

Fig. 8. Direct comparison of two different diameters of tubes, 1/4 and 1/2 in. o.d. with volume of 10 cm^3.

0.52 A/cm^2, for all the cases. Fig. 8 compares the different diameters of reservoir tubes for the 10 cm^3 volume. For the bigger tube diameter the undershoot/overshoot behavior is barely observable because the hydrogen/ambient air boundary is less defined at the end of the large diameter reservoir tube. The initial exit flowrate of hydrogen in the reservoir tube is 14.6 cm^3/min at the cell voltage of 0.7 V and thus the velocity of hydrogen in the 1/4 in. o.d. tube is 1.48 cm/s while that of 1/2 in. is 0.34 cm/s. This significantly slower velocity allows ambient air to flow into the tube so that the volume of hydrogen that reenters the cell after a voltage change from 0.7 to 0.5 V is less and this yields the shorter peak length for the larger diameter reservoir.

The response with a reservoir can be describe as a modified SO L/L system second-order plus dead time (SOPDT). The transfer function for this system is:

$$i(s) = \left[K_2 + \frac{K_1}{\tau^2 s^2 + 2\xi\tau s + 1} \mathrm{e}^{-\alpha s} \right] V(s) \quad (5)$$

The time domain function for this system can be described by the sum of two current densities, i_1 and i_2, where i_2 corresponds to the current density at the peak and during the peak length. Thus the peak length is modeled as a dead time α and the time dependent current after the peak length, i_1, applies to times after the dead time. The fitted parameters for each diameter and volume are listed in Table 4. The transient responses of this system are determined by damping coefficient, ξ, and the dead time, α. This SOPDT system explains the overshoot/undershoot behavior and peak length and it is an improvement to the analysis given in Reference [1]. Future work can now focus on a first principles description or model for damping coefficient, ξ, and the dead time, α.

4. Conclusions

Reservoir and dilution effects on dynamic behavior of a PEMFC fuel cell were studied at fixed flow rates of feed gases. The flowrates correspond to normal fuel and oxygen (air) utilization at the high cell voltage and a minimal operating condition at the low cell voltage. The results support the conclusion of our recent work [2] in that the increased velocity with diluted anode feed gas eliminates the "vacuum" effect and "undershoot" after overshoot behavior. Thus reformate fuel will yield less "undershoot" and less of a "vacuum" effect. The vacuum effect with neat hydrogen will provide local conditions of starvation due to a more non-uniform reaction rate during transient load changes. Also, the dilution effect affects the undershoot behavior in the current density recovery time when the initial voltage is 0.5 V (i.e., stoichiometry change from a 'starved' to a normal condition). The dilute fuel yields faster recovery time. We have shown that the volume of the reservoir influences the transient behavior of PEMFCs and thus, under proper design, the excess hydrogen in the manifold could serve the function of a capacitor and perhaps lower the need for a hybrid designs to handle the transient loads of the system. The ability to remove the battery/capacitor simplifies the system, may provide for increased reliability, and reduced cost.

The data also show that not just the volume of the reservoir but also the structure of the reservoir affects the transient behavior. The length and diameter of the reservoir affect the peak length as well as the undershoot after overshoot behavior. These ideas may lead one to better designs of flow fields so that the PEMFC can survive transient conditions. For example, changing the path length to the manifolds of fuel cell stack, may improve the response during unsteady operation.

Acknowledgements

Financial support by the South Carolina State University/University Transportation Center (Grant no. 2000–013), Department of Energy-EPSCoR (Cooperation Agreement DE-FG02-91ER75666), and Office of Naval Research, ONR (Grant no. N00014-98-1-0554) is gratefully acknowledged. The authors gratefully acknowledge that W.L. Gore & Associates, Inc. supplied the MEAs used in this work.

References

[1] S. Kim, S. Shimpalee, J.W. Van Zee, J. Power Sources (2004), in press.
[2] S. Kim, S. Shimpalee, J.W. Van Zee, J. Electrochem. Soc., submitted for publication.
[3] S. Shimpalee, W.-k. Lee, J.W. Van Zee, H. Naseri-Neshat, unpublished computations.
[4] S. Shimpalee, W-k. Lee, J.W. Van Zee, Presented at the 2002 Meeting of the Electrochemical Society, Philadelphia, PA, May 2002, paper #1136.
[5] J. Hamelin, K. Agbossou, A. Laperriere, F. Laurencelle, T.K. Bose, Int. J. Hydrogen Energy 26 (2001) 625–629.
[6] J.C. Amphlett, E.H. De Oliveria, R.F. Mann, P.R. Roberge, A. Rodrigues, J.P. Salvador, J. Power Sources 65 (1997) 173–178.
[7] B. Emonts, J. Bøgild Hansen, H. Schmidt, T. Grube, B. Hohlein, R. Peters, A. Tschauder, J. Power Sources 86 (2000) 228–236.
[8] R. Kötz, S. Müller, M. Bärtschi, B. Schnyder, P. Dietrich, F.N. Büchi, A. Tsukada, G.G. Scherer, P. Rodatz, O. Garcia, P. Barrade, V. Hermann, R. Gallay, in: G. Nazri, et al. (Eds.), Advanced Batteries and Supercapacitors, ECS Proceeding Volume, PV 2001–21 (2001).
[9] B.A. Ogunnaike, W.H. Ray, Process Dynamics, Modeling, and Control, Oxford, 1994, pp. 139–211.
[10] W.-k. Lee, C. Ho, J.W. Van Zee, J. Power Sources 84 (1999) 45–51.
[11] W.-k. Lee, Ph.D. dissertation, Department of Chemical Engineering, University of South Carolina, SC, 29208, 1999, pp. 16–21.